https://doi.org/10.5194/acp-2022-696
Preprint. Discussion started: 4 October 2022

Atmospheric Chemistry and Physics Discussions

The Chance of Freezing – Parameterizing temperature dependent freezing including randomness of INP concentrations

Hannah C. Frostenberg[1], André Welti[2], Mikael Luhr[3], Julien Savre[4], Erik S. Thomson[5], and Luisa Ickes[1]

[1]Department of Space, Earth and Environment, Chalmers University, Gothenburg 41296, Sweden
[2]Finnish Meteorological Institute, Helsinki 00101, Finland
[3]former Department of Meteorology, Stockholm University, Stockholm 10691, Sweden
[4]Meteorological Institute, Faculty of Physics, Ludwig-Maximilians-Universität, Munich 80333, Germany
[5]Department of Chemistry and Molecular Biology, University of Gothenburg, Gothenburg 41296, Sweden

Correspondence: Hannah Frostenberg (hannah.frostenberg@chalmers.se), Luisa Ickes (luisa.ickes@chalmers.se)

Abstract. Ice nucleating particle (INP) concentrations can spread over several orders of magnitude at any given temperature. However, this variability is rarely accounted for in heterogeneous ice nucleation parameterizations. We developed a scheme for immersion freezing where the INP concentration is drawn from a relative frequency distribution of cumulative INP concentrations. At each temperature, this distribution describing the INP concentrations is expressed as a log-normal frequency distribution. The new parameterization scheme does not require aerosol information from the driving model to represent the heterogeneity of INP concentrations. The scheme's performance is tested in a large-eddy simulation of an Arctic stratocumulus. We find that it leads to reasonable ice masses in the cloud. The scheme is sensitive to the median of the frequency distribution and highly sensitive to the standard deviation of the distribution. Generally, larger probability to draw high INP concentrations leads to substantially more ice in the simulated cloud.

1 Introduction

Clouds play an important role in Earth's energy balance by reflecting incoming sunlight and interacting with infrared radiation. The cloud phase influences the amount of a cloud's radiative effect, but more importantly it determines whether the cloud has a warming or cooling effect. According to Matus and L'Ecuyer (2017), liquid clouds have a global net radiative effect at top-of-atmosphere (TOA) of -11.8 W m^{-2}, whereas ice clouds exert a warming of 3.5 W m^{-2} and mixed-phase clouds cause a net cooling effect of -3.4 W m^{-2}.

The ice crystals in mixed-phase clouds usually originate from heterogeneous ice nucleation where ice nucleating particles (INPs) are necessary to trigger the phase transition. Ice nucleates heterogeneously in the atmosphere for temperatures between 0 and approximately -38°C. At temperatures below -38°C, homogeneous ice nucleation occurs spontaneously and freezing can happen without INPs. Heterogeneous ice nucleation can occur in different so-called modes. We focus on immersion freezing where an INP is immersed in a supercooled cloud droplet and initiates freezing at a specific temperature. Contact freezing, deposition nucleation and condensation freezing are further heterogeneous nucleation modes (see Vali et al., 2015, for definitions). Different aerosol types can act as INPs: mineral dusts, biological and combustion particles, etc. The probability that

https://doi.org/10.5194/acp-2022-696
Preprint. Discussion started: 4 October 2022


Atmospheric Chemistry and Physics Discussions

an aerosol initiates ice nucleation increases with decreasing temperature. Measurements of ambient INP concentrations (INPC [m^{-3}]) show that at a given temperature, INPC can vary by several orders of magnitude, over time and space. An example for spatial INPC variability in different marine locations, from approximately 10^{-1} to 10^{3} m^{-3} at -15°C can be found in Welti et al. (2020). Temporal variability, for example the annual cycle of INPC in the Arctic, was reported to be up to three orders of magnitude (Wex et al., 2019). But also within smaller time periods down to single days, the INPC can fluctuate by up to three orders of magnitude (Bigg, 1961).

Several parameterizations that simulate cloud droplet freezing exist and they are based on different physical variables. Burrows et al. (2022) distinguish between aerosol-aware and -unaware parameterizations. One example of the latter is the formulation by Fletcher (1962) (F62); a scheme that only requires temperature information to calculate INPC. F62 is based on the observation that while the INPC varies from day to day and place to place, the average concentration increases exponentially with decreasing temperature for -10 $> T >$ -30°C. The scheme by Niemand et al. (2012) (N12) is an example of an aerosol-aware parameterization, since it describes immersion freezing based on the active site density of desert dust aerosols observed in laboratory measurements. N12 is valid from -12 to -36°C and requires the number of dust aerosols, the average INP surface and temperature as input to determine INPC. Another example of an aerosol-aware scheme is the parameterization by Phillips et al. (2008) (P08) which represents immersion, contact and deposition freezing on dust/metal aerosol, organic carbon and biological INPs. P08 uses temperature, water vapour saturation with respect to ice and aerosol concentrations of the four aerosol species to predict INPC. P08 is valid for temperatures between 0 and -70°C (or lower). The parameterization of Khvorostyanov and Curry (2000) (K00) is based on classical nucleation theory (CNT), where each substance is assigned a characteristic contact angle between a nucleating ice cluster and the particle surface. The smaller the contact angle, the more ice active a substance. K00 utilizes temperature, water vapour saturation with respect to ice, particle radius and one contact angle per substance to calculate ice nucleation rates. One method of including particle to particle heterogeneity of INPs in parameterizations is to apply a distribution on the contact angle parameter in CNT to calculate the ice-activity of the INPs (e.g., Marcolli et al., 2007 or Wang et al., 2014). These schemes use temperature and aerosol size distributions as input from the atmospheric model and use different values for the mean and standard deviation of the contact angle distribution for different aerosol species. There are three drawbacks that ice nucleation parameterizations can have: i. They can be computationally complex, i.e., require detailed input from the model regarding aerosol type, size and/or number concentration. ii. They often are valid only for a limited temperature range. iii. They fail to reproduce INPC variability, i.e., for one set of environmental conditions (temperature, humidity, aerosol type and concentration) they yield one fixed INPC value.

The lack of INPC variability in simulations compared to atmospheric observations comes from the large size of model grid boxes and the use of bulk aerosol concentrations (e.g., dust, soot, biological) as input variables in parameterizations. Even if a model had information on, e.g., the detailed size distribution of dust aerosol, it will not represent all the different dust INP types (different minerals) and their variability that are present in the atmosphere. To circumvent these drawbacks we developed a parameterization of immersion freezing (F22) that simulates observed INPC and their variability while only using temperature as input variable. F22 is valid for the entire temperature range of immersion freezing (from 0 to -38°C). The INPCs returned by F22 are drawn randomly from a log-normal distribution of INPCs for each temperature, thereby capturing the natural INP

https://doi.org/10.5194/acp-2022-696
Preprint. Discussion started: 4 October 2022

Atmospheric Chemistry and Physics Discussions

variability, without information about the present bulk aerosol. Log-normal distributions of INPCs have been observed at several locations with different environments (e.g., Isaac and Douglas, 1971; Bertrand et al., 1973; Radke et al., 1976; Flyger and Heidam, 1978; Conen et al., 2017; Welti et al., 2018; Hartmann et al., 2019; Schrod et al., 2020; Li et al., 2022). The similarity to a log-normal distribution indicates that the measured INPCs were subject to random dilutions since their emission into the atmosphere (Ott, 1990). The log-normal distribution F22 is based upon has been found in observations in the maritime boundary layer (see Sec. 2).

We tested the performance of the new F22 parameterization in the large-eddy simulation (LES) model MIMICA (MISU/MIT Cloud-Aerosol model, Savre et al., 2014) to confirm that it produces a reasonable amount of ice in a simulated cloud and analyzed the sensitivity of the scheme. The simulations are initialized based on observations during the ASCOS Arctic campaign and represent a mixed-phase stratocumulus with in-cloud temperatures between approximately -7 and -10°C (see Sec. 2.2).

2 Method

2.1 Formulation of the F22 parameterization

The F22 parameterization for immersion freezing is based on i. a long-term time series of INPC temperature spectra measured in the maritime boundary layer at Cabo Verde (Welti et al., 2018) and ii. wide-area ship-based observations (Welti et al., 2020). The observations were made by collecting INPs on filters and subsequent drop freezing experiments at temperatures from 0 to -26°C, and using a continuous flow diffusion chamber for low-temperature observations (-24 to -38°C). On average there is a striking consistency of the temperature spectra's shape and variability over time and location. The same consistencies exist in comparison with other long-term or composite INPC data sets (e.g. Petters and Wright, 2015).

Based on the aforementioned data sets, we derived a function for temperature-dependent, log-normally distributed INPC frequency:

$$D(\mu,\sigma^2) = \frac{1}{\sqrt{2\pi}\cdot\sigma}\exp\left(-\frac{\left[\ln(\mathrm{INPC})-\mu\right]^2}{2\sigma^2}\right), \tag{1}$$

with $\mu(T)$ the temperature dependent mean and σ^2 the variance of the log-normal distribution (not the INPC itself). For the marine data sets we find $\sigma = 1.37$ and $\mu(T) = \ln(-T^9 \cdot 10^{-9})$ with T given in °C. By normalizing the distribution, a relative frequency distribution (RFD) as function of temperature is obtained (Fig. 1). Whenever a freezing event occurs in the model (i.e., $T \leq 0°\mathrm{C}$ and saturation with respect to ice, $s_i \geq 1$), an INPC value is drawn randomly from the RFD. That is, for two grid points with freezing events at the same temperature, the drawn INPC can differ by several orders of magnitude. For a large number of grid points, the relative frequency of the drawn INPC will follow a log-normal function with the median INPC (orange region in Fig. 1) having the highest probability. For example, if all grid points had the temperature -16°C, the frequency of the picked INPC would follow the green curve shown in the lower left Fig. 1 inset.

F22 assumes that all INPs are immersed in cloud droplets. To take into account the dynamic evolution of ice formation, the ice crystal number concentration (N_i) at the grid point is subtracted from the drawn INPC. This returns the number of newly

https://doi.org/10.5194/acp-2022-696
Preprint. Discussion started: 4 October 2022

Atmospheric Chemistry and Physics Discussions

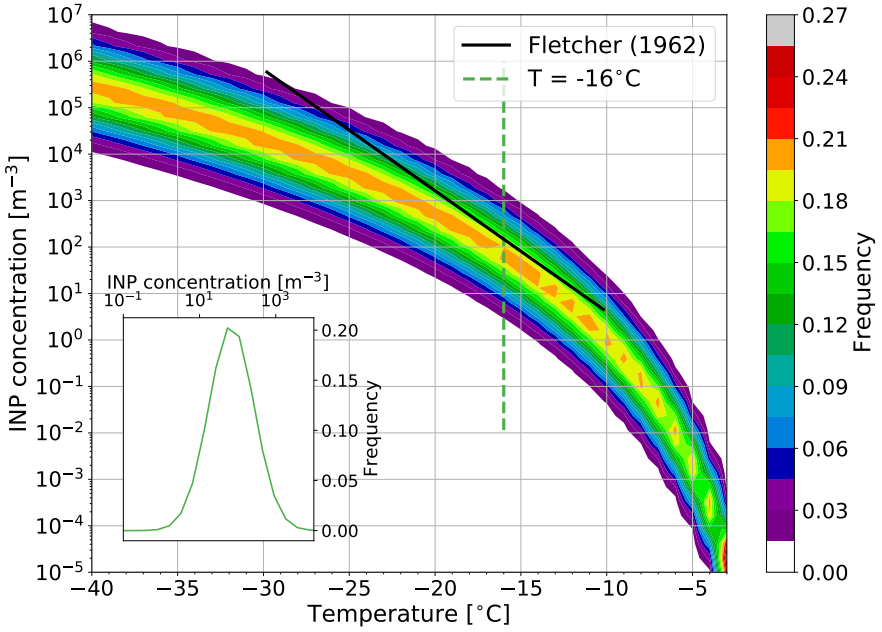

Figure 1. Relative frequency distribution spectra for INPC as a function of temperature. The log-linear parameterization by Fletcher (1962) within its validity range is shown for comparison. The inset in the lower left corner shows the RFD at $T = -16$ °C (dashed line).

frozen cloud droplets in the time step, i.e., hydrometeors moving from class *cloud droplet* to class *ice crystal*. No negative tendencies are allowed in the scheme, since already frozen cloud droplets will not melt due to a decrease in INPs. The change in the respective mixing ratios is calculated by multiplying by the average cloud droplet mass:

$$\Delta N_i = -\Delta N_c = \max([\mathrm{INPC} - N_i], 0), \tag{2a}$$

$$\Delta Q_i = -\Delta Q_c = \Delta N_i \frac{\overline{Q_c}}{\overline{N_c}}. \tag{2b}$$

Here, N_i and N_c are the ice crystal and cloud droplet number concentrations, respectively, Q_i and Q_c are the ice crystal and cloud droplet mixing ratios, respectively, and the mean cloud droplet mixing ratio and number concentration are denoted by the bar. The calculations are repeated at each time step, which means that INPs are only partially depleted through the subtraction of N_i. We see this as a way to imitate time dependent freezing and INP cycling, which has been shown to be crucial for realistic cloud development in LES for Arctic mixed-phase clouds (e.g., Solomon et al., 2015).

The implemented INPC RFD-field is discretized into bins of INPC and temperature. The INPCs differ approximately by a factor of 2 (or $\Delta \log_{10}(\mathrm{INPC}) \approx \log_{10}(2)$), while the temperature bins have a size of 1°C. This is why we define temperature to the nearest degree when drawing from the INPC RFD if not stated otherwise.

https://doi.org/10.5194/acp-2022-696
Preprint. Discussion started: 4 October 2022

Atmospheric Chemistry and Physics Discussions

2.1.1 Example of parameterized INP concentrations

To illustrate the INPC distribution from the F22 parameterization, let us assume that we have a uniform -16°C cloud horizontally spreading over the entire model domain consisting of 1000 grid points. In this case, the INPC RFD at all cloud grid points is represented by a log-normal distribution curve (inset in Fig. 1). That means that an INPC of approximately 68.7 m^{-3} will be drawn with the highest probability, since this is the median INPC: $\mathrm{Med}[\mathrm{INPC}(T = -16°\mathrm{C})] = \exp(\mu) = -T^9 \cdot 10^{-9} \approx 68.7\,\mathrm{m}^{-3}$. 20.2% of the grid points will draw the median INPC, so 202 of the 1000 cloud grid points are expected to get the median INPC of 54.3 m^{-3} (differing from the theoretical value of 68.7 m^{-3} because of discrete INPC bins). The range of INPC bins with a relative frequency $> 0.1\%$ covers 0.8 - 7543.1 m^{-3}, which means that neither INPCs ≤ 0.8 nor ≥ 7543.1 m^{-3} will be drawn in the example cloud. If no ice was present previously, the INPC equals the number of cloud droplets frozen at this time step (Eq. 2a), limited by the total number of cloud droplets present.

2.1.2 Representing the RFD

Since the parameterization draws values from a distribution, it needs to be ensured that there are enough random draws at each time step in order to represent the distribution well: INPCs in the model should vary according to the distribution, but different model runs should also be reproducible. To investigate how many draws are necessary for a "good" representation of the INPC-distribution, we conducted several drawing tests (drawing, e.g., 50 times from the distribution vs. drawing 100 times) at -16°C and compared the relative frequencies of the drawn values to the theoretical ones by calculating the root mean square error (RMSE) between the drawn and theoretical distributions. Comparing the results of the different drawing tests suggests that 300 random draws lead to a reproducible prediction of the RFD (see Table 1 and Fig. 2); the RMSE converges for ≥ 300 with a constant first derivative of the connecting lines, and the standard deviation decreases only slightly for > 300 draws.
The domain used in the simulations has 96×96 grid points in the horizontal, leading to 9 216 grid points in each layer. The simulated cloud is stratocumulus (see Sec. 2.2), where the temperature field is very uniform in the horizontal. Assuming that at least one layer of grid points in the model has the same temperature due to the uniform structure of the stratus cloud, this translates into a minimum of 9 216 grid points with the same temperature. This implies a minimum of 9 216 draws from the RFD at one temperature, which is substantially more than the minimum number of draws determined to well-represent the distribution (300). Hence, we confirm that a representative INPC distribution is being drawn from the RFD.

2.1.3 Performance of the parameterization scheme in MIMICA

Using the F22 immersion freezing scheme approximately doubles the computational expense compared to the standard MIMICA setup where ice nucleation is not represented explicitly, i.e., runs without an explicit freezing parameterization (instead the ice crystal number concentration (N_i) is kept constant). The computational expense of applying F22 is similar to using other freezing parameterizations like N12 (Niemand et al., 2012).

https://doi.org/10.5194/acp-2022-696
Preprint. Discussion started: 4 October 2022

Atmospheric Chemistry and Physics Discussions

Table 1. Average and standard deviation of RMSE for different draw amounts from the INPC RFD at -16°C compared to theoretical RFD values. Each drawing test was performed 100 times and the table contains the average and standard deviation of the RMSE over these 100 times.

Number of draws	Mean RMSE [m^{-3}]	Standard deviation RMSE [m^{-3}]
50	$17.8 \cdot 10^{-3}$	$5.47 \cdot 10^{-3}$
100	$12.4 \cdot 10^{-3}$	$3.51 \cdot 10^{-3}$
200	$8.65 \cdot 10^{-3}$	$2.58 \cdot 10^{-3}$
300	$7.28 \cdot 10^{-3}$	$2.03 \cdot 10^{-3}$
400	$6.26 \cdot 10^{-3}$	$1.59 \cdot 10^{-3}$
500	$5.67 \cdot 10^{-3}$	$1.40 \cdot 10^{-3}$
600	$5.27 \cdot 10^{-3}$	$1.49 \cdot 10^{-3}$
700	$4.77 \cdot 10^{-3}$	$1.39 \cdot 10^{-3}$
800	$4.45 \cdot 10^{-3}$	$1.19 \cdot 10^{-3}$
900	$4.18 \cdot 10^{-3}$	$1.08 \cdot 10^{-3}$
1000	$3.73 \cdot 10^{-3}$	$1.11 \cdot 10^{-3}$

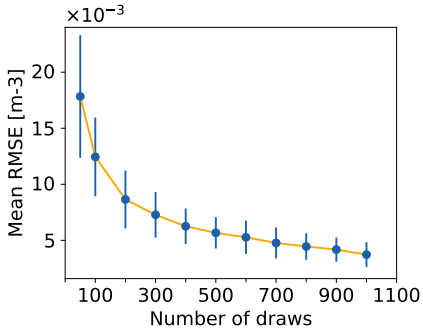

Figure 2. Average and standard deviation of RMSE for the drawing tests in Table 1 are decreasing for increasing number of draws at -16°C.

2.2 Simulation setup

We use the well-established large-eddy simulation (LES) model MIMICA (MISU/MIT Cloud-Aerosol model, Savre et al., 2014). For more information on the model, see additionally Appendix A or, e.g., Savre and Ekman (2015a), Savre and Ekman (2015b), or Sotiropoulou et al. (2020). The simulated case is based on a mixed-phase Arctic stratocumulus. The case-study stratocumulus cloud was observed between 30 August and 31 August 2008 during the ship-based ASCOS campaign (Arctic Summer Cloud Ocean Study; Tjernström et al., 2014). At that time, the research vessel Oden was drifting with an ice-floe located at approximately 87 °N. The atmospheric conditions were characterized by a high-pressure system with large-scale subsidence in the free troposphere (for details see Tjernström et al., 2012). This case has been used to study other microphysical cloud properties like dissipation (Loewe et al., 2017), the influence of CCN hygroscopicity on cloud properties (Christiansen et al., 2020), secondary ice production (Sotiropoulou et al., 2021) and sustenance (Bulatovic et al., 2021) of an Arctic mixed phase cloud, as well as in a model intercomparison study (Stevens et al., 2018). We selected this case, because there are large

https://doi.org/10.5194/acp-2022-696
Preprint. Discussion started: 4 October 2022


Atmospheric Chemistry and Physics Discussions

uncertainties about the nature and concentration of INPs in the Arctic, which poses a challenge to modeling mixed-phase clouds in this region. Using other immersion freezing parameterizations in MIMICA, for example an active site scheme following Ickes et al. (2017), to simulate this case requires unrealistically active INPs in order to form ice. Simulations of the case without interactive ice nucleation (STD) assume a constant ice crystal number concentration of 200 m^{-3} at grid points with a temperature below 0°C where the supersaturation ratio with respect to ice is at least 0.05 and where there are sufficient cloud droplets. This means that at any given time step, if N_i falls below 200 m^{-3}, cloud droplets are converted to ice to retain $N_i = 200$ m^{-3}.

The MIMICA simulations are initialized with the profiles of thermodynamic variables (e.g., potential temperature and pressure) and liquid cloud water that were measured at approximately 06 UTC on 31 August 2008. A cloud layer was present between ca. 550 and 900 m above ground level, capped by a temperature and humidity inversion and de-coupled from the surface (see Sotiropoulou et al., 2021 for profile details). The temperature within the cloud ranged from approximately -7 to -10°C. The simulation setup follows Sotiropoulou et al. (2021). The domain covers a $96 \times 96 \times 128$ grid with constant horizontal spacing of $dx = dy = 62.5$ m (6 km×6 km horizontal domain size). The vertical spacing is 7.5 m near the ground and in the cloud layer; between the surface and the cloud it changes sinusoidally and reaches a maximum dz of 25 m, with a 1.7 km total vertical domain size. The time step is dynamic in order to satisfy the Courant-Friedrichs-Levy (CFL) condition for the leapfrog time-integration method and ranges from $\approx$ 1 - 3 s to prevent numerical instabilities within the model. Our simulations cover 12 hours, with the first two hours utilized as a spin-up period and subsequently omitted from the results. A large-scale steady state is maintained throughout the model runs and the cloudy layer is present in the initial state of the simulations. However, the initial cloud is liquid and cloud ice is only formed from the first model time step.

We excluded the hydrometeor categories snow and graupel from our simulations, since it is known that MIMICA produces rather large amounts of graupel for this case (Stevens et al., 2018) which dominates both ice water path (IWP) and the number concentration of frozen hydrometeors. Because we are primarily interested in ice formation in our study, ice crystals being the only frozen hydrometeors simplifies the analysis. For the same reason, snow and graupel were excluded previously from Arctic stratocumulus simulations conducted with MIMICA (Savre and Ekman, 2015b). Excluding snow and graupel means that no cold collection processes are active in our simulations. Aerosol is not represented prognostically in the model setup.

For comparisons of simulations with MIMICA of the 30 - 31 August 2008 ASCOS case to observations, we refer to Sotiropoulou et al. (2021) and Stevens et al. (2018).

3 Results and discussion

We first compare the baseline version of the new F22 parameterization (F22, all parameters are set to the values described in Sect. 2.1 and Sect. 2.2) to the standard setup (STD).

Domain-averaged liquid water path (LWP [g m^{-2}]), ice water path (IWP [g m^{-2}]), ice crystal number burden (ICNB [m^{-2}]) and net infrared radiation at the surface (NIRS [W m^{-2}]) for STD and F22 are shown in Fig. 3. The model was run using STD or F22 ten times, respectively. In Fig. 3, the different "ensemble members" are represented by their median, maximum and

https://doi.org/10.5194/acp-2022-696
Preprint. Discussion started: 4 October 2022

Atmospheric Chemistry and Physics Discussions

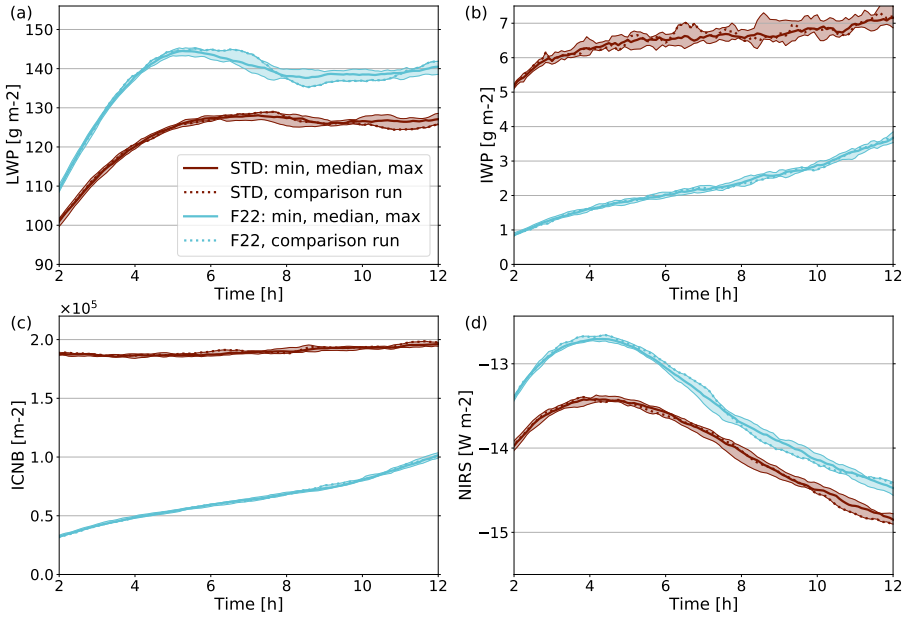

Figure 3. Domain-averaged **(a)** LWP, **(b)** IWP, **(c)** ice crystal number burden (ICNB) and **(d)** net infrared radiation at surface (NIRS) for 10 simulations of STD (red; median with min/max envelope) and with the F22 parameterization (cyan; median with min/max envelope). In both cases one representative simulation is plotted as dotted line to be included in Figs. 4, 6, 8, 10, 12, B1.

minimum values.

LWP is substantially larger for F22 than for STD (Fig. 3a). The vertical distributions of N_c and Q_c (Fig. B1b and d) are very similar between STD and F22, which indicates that the differences in LWP are mainly caused by differences in the amount of rain drops. IWP is larger for STD than for F22 (Fig. 3b), but does not compensate the differences in LWP (the total mass of ice and liquid is still larger for F22). The large differences in LWP between F22 (INPC distribution) and STD (constant N_i) are due to enhanced freezing in STD, which leads to more latent heat release, increasing temperature and lowering supersaturation. This causes evaporation of liquid droplets, either with a mass flux to ice crystals via the Wegener-Bergeron-Findeisen process (WBF) or to the gas-phase. Another cause might be a difference in turbulence with more entrainment of drier air for STD.

To analyze the ice crystal number, Fig. 3c shows the ice crystal number burden (ICNB), the vertically integrated N_i. For STD, ICNB is almost constant at $1.9 \cdot 10^5$ m^{-2}, while it increases throughout the F22 simulations from $3.5 \cdot 10^4$ m^{-2} to almost $1.0 \cdot 10^5$ m^{-2}. ICNB has a similar slope as F22 IWP, suggesting that the average ice crystal mass remains constant throughout the F22 simulations. Comparing IWP and ICNB for STD, the average ice crystal mass increases throughout the simulation leading to different cloud situations.

Figure 3d shows the time series of the net infrared radiation at the surface (NIRS), i.e., incoming minus outgoing infrared radiation. NIRS is larger for F22 compared to STD. This can be expected since LWP is larger for F22. The evolution over time is similar in both cases, with NIRS first increasing, then decreasing from hours 4-5. This pattern emerges from the combination

https://doi.org/10.5194/acp-2022-696
Preprint. Discussion started: 4 October 2022

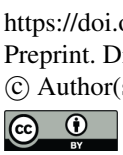

Atmospheric Chemistry and Physics Discussions

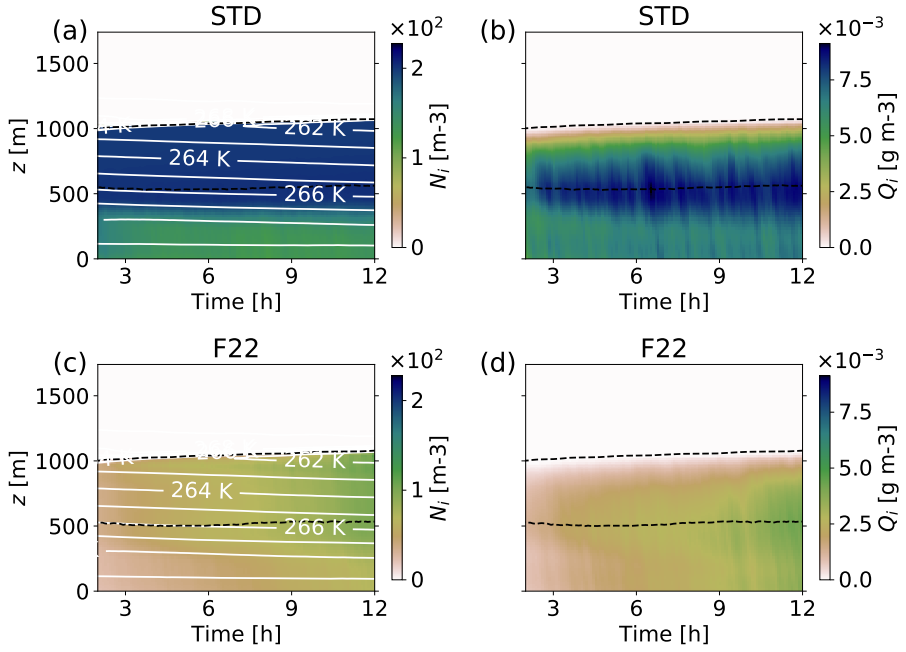

Figure 4. Domain-averaged profiles for simulation time after 2 hour spinup-time: **(a)** and **(c)** N_i with contours of temperature, **(b)** and **(d)** ice mixing ratio (Q_i). Upper row (**a**, **b**) is the STD comparison run (see dotted lines in Fig. 3), lower row (**c**, **d**) is the F22 comparison run (see dotted lines in Fig. 3). The dashed lines show the cloud top and bottom.

of first increasing, then steady LWP (for F22, LWP decreases slightly between hours 5 and 8, which causes a larger decrease in NIRS), and continuously decreasing temperature (not shown) due to radiative cooling of the cloud.

The variability between different realizations of either STD or F22 is shown in Fig. 3. For IWP (Fig. 3b), STD values have a larger spread than F22, while their spread is similar for the other variables. Since in STD, the ice crystal number concentration is set to a constant value where certain conditions for the temperature and supersaturation are met, fluctuations due to randomly perturbed initial conditions can have a larger effect. If several grid points are close to the supersaturation threshold, small perturbations can either cause the threshold to be exceeded and thus N_i set to 200 m^{-3}, or not to be exceeded resulting in no adaptation of N_i. This leads to a rather variable IWP for different STD runs. In contrast, for F22 the variation between the drawn INPCs at different grid points can be large in any simulation, because a large number of freezing events happens at each time step. Overall, this results in a more stable IWP between different realizations.

The profile of N_i for STD in Fig. 4a illustrates the principle of that immersion freezing representation: for STD, within the cloud and ca. 100 m below it, N_i has the prescribed value of 200 m^{-3}. Down to the surface, the concentration is lower but constant, which is caused by steady sedimentation of ice crystals from above combined with fewer grid points reaching the threshold ice supersaturation. Q_i has the maximum values at the cloud bottom (Fig. 4b). Since no cold-phase collection processes are active in these simulations, ice crystal mass can only grow by deposition. The vertical distribution of N_i and Q_i

https://doi.org/10.5194/acp-2022-696
Preprint. Discussion started: 4 October 2022

Atmospheric Chemistry and Physics Discussions

Table 2. Overview of sensitivity studies

Simulation name	Abbreviation	Frequency of drawing from RFD	Horizontal grid spacing	Minimum vertical grid spacing	Multiplicator of RFD Median	RFD Standard deviation	Size of temperature-bins
standard[a]	STD	-	62.5 m	7.5 m	-	-	-
baseline F22	F22	every Δt[b]	62.5 m	7.5 m	1	1.37	1°C
median 1.5	M1.5	every Δt	62.5 m	7.5 m	1.5	1.37	1°C
median 1.25	M1.25	every Δt	62.5 m	7.5 m	1.25	1.37	1°C
median 0.75	M0.75	every Δt	62.5 m	7.5 m	0.75	1.37	1°C
median 0.5	M0.5	every Δt	62.5 m	7.5 m	0.5	1.37	1°C
sigma 1.5	S1.5	every Δt	62.5 m	7.5 m	1	1.5·1.37	1°C
sigma 1.25	S1.25	every Δt	62.5 m	7.5 m	1	1.25·1.37	1°C
sigma 0.75	S0.75	every Δt	62.5 m	7.5 m	1	0.75·1.37	1°C
sigma 0.5	S0.5	every Δt	62.5 m	7.5 m	1	0.5·1.37	1°C
sigma 0	S0	-	62.5 m	7.5 m	1	-[c]	1°C
half degree	0.5Deg	every Δt	62.5 m	7.5 m	1	1.37	0.5°C
once 5 sec	5S	once per 5 sec	62.5 m	7.5 m	1	1.37	1°C
once 10 sec	10S	once per 10 sec	62.5 m	7.5 m	1	1.37	1°C
once 20 sec	20S	once per 20 sec	62.5 m	7.5 m	1	1.37	1°C
once 5 min	5M	once per 5 min	62.5 m	7.5 m	1	1.37	1°C
once 60 min	60M	once per 60 min	62.5 m	7.5 m	1	1.37	1°C
low resolution	F22 LR	every Δt	125 m	15 m	1	1.37	1°C

[a] Simulation with fixed N_i, no interactive ice nucleation parameterization
[b] Time step
[c] In this case no distribution is used, but the median of the distribution for all freezing cases

in F22 is similar to STD (Fig. 4c and d). However, both Q_i and N_i increase by larger rates throughout the simulation time for F22, which can also be seen in the IWP values (Fig. 3b). Towards the end of the simulation time, F22 ice values are about half of STD. Even though ice nucleation depends on temperature in F22, N_i is quite homogeneously distributed throughout the cloud (Fig. 4c). We explain this by the subtraction of N_i from INPC (Eq. 2a) in the scheme, which homogenizes N_i vertically over time.

3.1 Sensitivity studies

To investigate the sensitivity of the simulated cloud to the characteristics of the F22 scheme, the following parameters (summarized in Tab. 2) were varied: i. the median and standard deviation of the INPC distribution (Secs. 3.1.1 and 3.1.2); ii. the size of the temperature bins (Sec. 3.1.3); iii. the frequency of drawing (Sec. 3.1.4); iv. the resolution of the model domain (Sec. 3.1.5).

3.1.1 Median of the distribution

The median ($\exp(\mu)$) of the INPC RFD is multiplied by a factor (0.5-1.5) shifting the entire distribution in Fig. 1 up or down, without changing the standard deviation. Having more INPs (higher median) or fewer INPs (lower median) impacts the amount of ice formed in the cloud. The effect can be seen from the modeling results of IWP (Tab. 3; Fig. 5), when increasing/decreasing the median by 25% or 50%, IWP increases/decreases accordingly. The vertical profiles exhibit this symmetry even more clearly

https://doi.org/10.5194/acp-2022-696
Preprint. Discussion started: 4 October 2022

Atmospheric Chemistry and Physics Discussions

Table 3. The three quartiles (25th percentile: P_{25}, etc.) of IWP for all sensitivity studies for the final four simulationed hours (8-12 h) and differences relative to F22 (ΔF22) or STD (ΔSTD). Values in g m^{-2}. Simulations with significant differences to F22 (STD) are highlighted with an asterisk. Significance was assessed with a two-sided Kolmogorov-Smirnov test at the 95% level.

Simulation	**IWP P_{25}**	ΔF22/ ΔSTD	**IWP P_{50}**	ΔF22/ ΔSTD	**IWP P_{75}**	ΔF22/ ΔSTD
F22	2.6	-	2.8	-	3.3	-
M1.5 *	3.7	1.1	4.0	1.2	4.8	1.5
M1.25 *	3.4	0.8	3.5	0.7	4.0	0.7
M0.75 *	2.0	-0.6	2.2	-0.6	2.4	-0.9
M0.5 *	1.4	-1.2	1.5	-1.3	1.7	-1.6
S1.5 *	16.8	14.2	17.3	14.5	18.1	14.8
S1.25 *	7.3	4.7	7.8	5.0	8.7	5.4
S0.75 *	0.9	-1.7	1.0	-1.8	1.2	-2.1
S0.5 *	0.4	-2.2	0.4	-2.4	0.5	-2.8
S0 *	0.1	-2.5	0.1	-2.7	0.1	-3.2
0.5Deg	2.6	-	3.0	0.2	3.3	-
5S *	2.1	-0.5	2.2	-0.6	2.6	-0.7
10S *	1.8	-0.8	1.9	-0.9	2.1	-1.2
20S *	1.5	-1.1	1.7	-1.1	1.9	-1.4
5M *	1.2	-1.4	1.3	-1.5	1.5	-1.8
60M *	1.2	-1.4	1.3	-1.5	1.4	-1.9
F22 LR *	1.8	-0.8	1.9	-0.9	2.3	-1.0
STD	6.7	-	6.8	-	7.0	-
STD LR *	6.3	-0.4	6.5	-0.3	6.7	-0.3

with linear N_i and Q_i increases/decreases (Fig. 6a and b) and all changes are significant. The significance of differences in IWP between simulations is tested with a two-sided Kolmogorov-Smirnov test at the 95% level. Changes in vertical profiles are tested with a two-sided t-test at the 95% level. It is expected that all variables concerning ice crystals increase (decrease) with increased (decreased) median INPC, since more (fewer) INPs lead to more (fewer) cloud droplets freezing. The change is linear, since the median is logarithmized in the formula's exponent (see Eq. 1). No change in the vertical distribution of cloud droplet concentration is apparent (not shown).

3.1.2 Standard deviation of the distribution

The standard deviation (σ) of the RFD determines the variability of the INP concentration. The wider the distribution, the larger the variability of drawn INPCs. For the modeled cloud, a larger variability results in substantially and significantly increased

https://doi.org/10.5194/acp-2022-696
Preprint. Discussion started: 4 October 2022

Atmospheric Chemistry and Physics Discussions

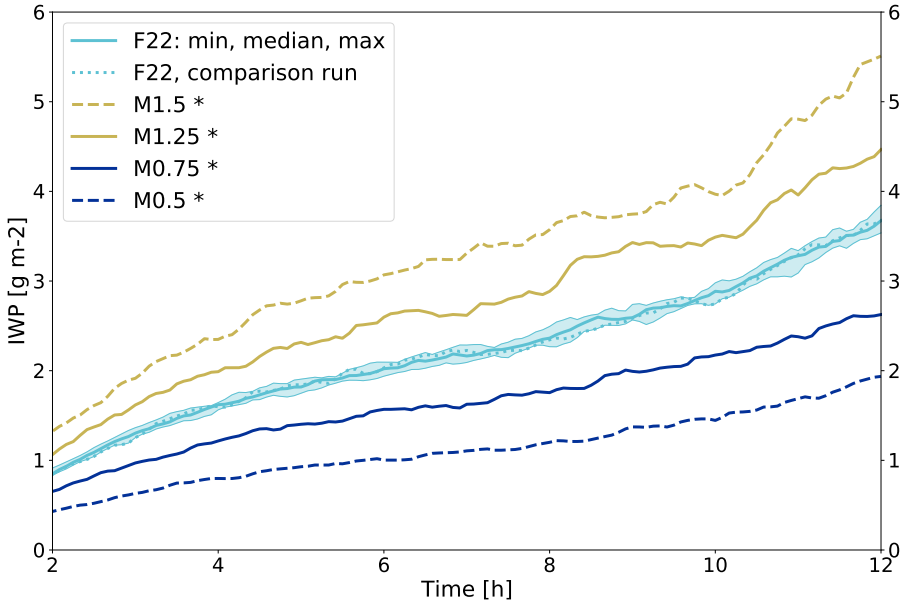

Figure 5. Domain-averaged IWP for 10 F22 simulations (cyan; median with min/max envelope, comparison run used in Fig. 6 is shown as dotted line). Four sensitivity runs where the median of the RFD was changed (yellow: higher median INPC, blue: lower median INPC). Significance was assessed with a two-sided Kolmogorov-Smirnov test at the 95% level. Significant differences to F22 are marked with an asterisk.

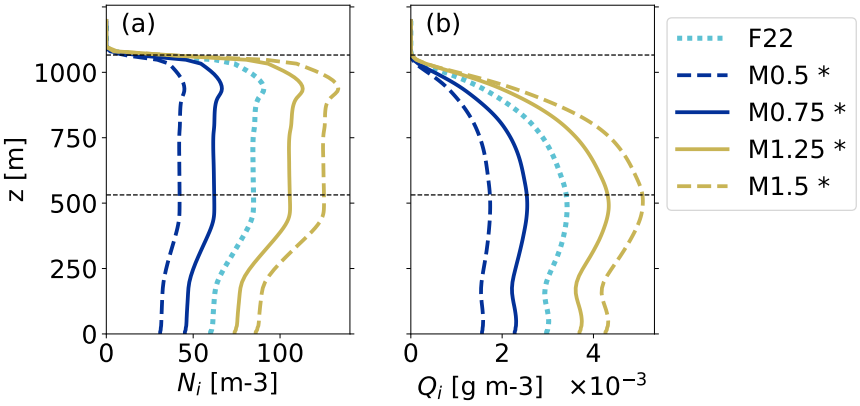

Figure 6. Profiles averaged over the domain and the simulation period of 8 - 12 hours: **(a)** N_i, **(b)** Q_i. The F22 comparison run is plotted in dotted cyan (see dotted line in Fig. 5), M0.5 and M0.75 in blue and M1.25 and M1.5 in yellow. Simulations with significant differences compared to F22 are marked with an asterisk (tested with a two-sided t-test at the 95% level). Horizontal dashed lines indicate the cloud top and bottom in F22.

https://doi.org/10.5194/acp-2022-696
Preprint. Discussion started: 4 October 2022

Atmospheric Chemistry and Physics Discussions

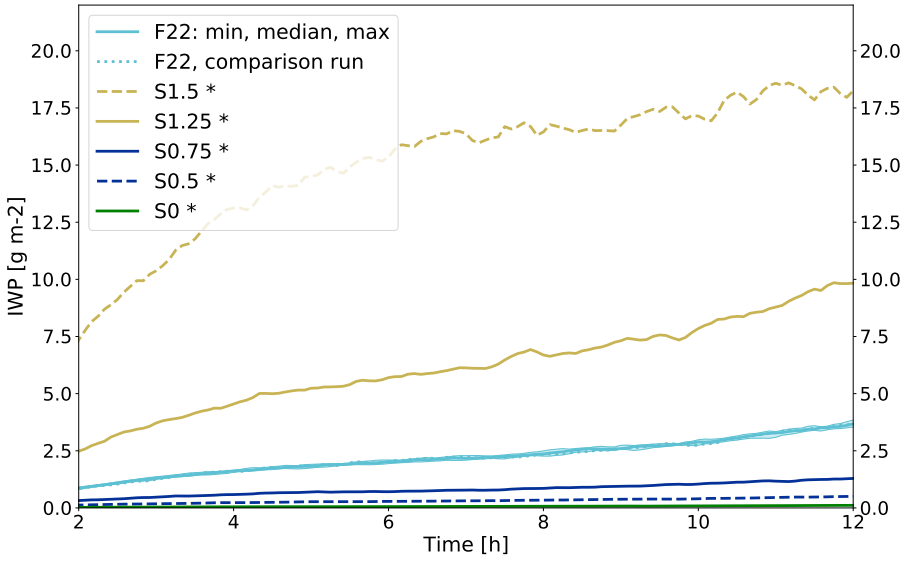

Figure 7. Domain-averaged IWP for 10 F22 simulations (cyan; median with min/max envelope, comparison run used in Fig. 8 is shown as dotted line). Five sensitivity runs where the standard deviation of the RFD was changed (yellow: larger standard deviation, blue: smaller standard deviation, green: no standard deviation (Only median, M)). Significant differences to F22 are marked with an asterisk.

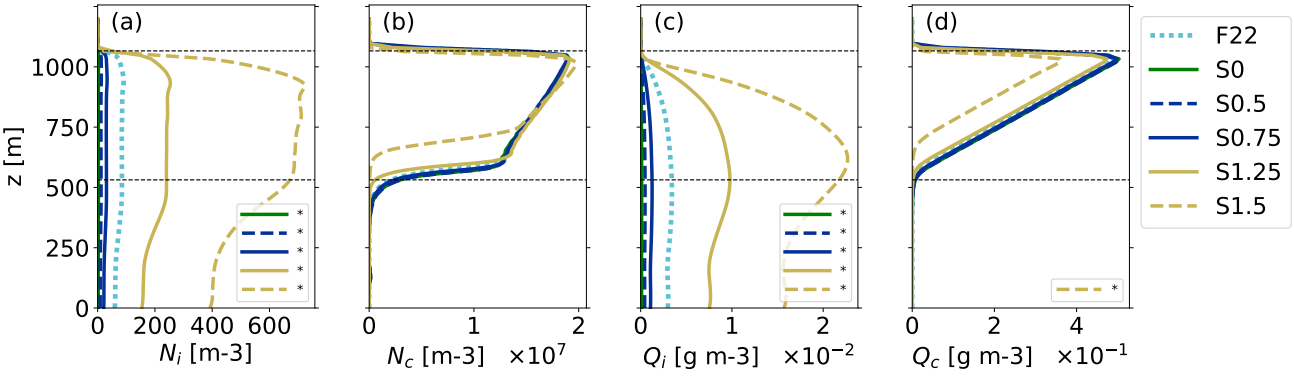

Figure 8. Profiles averaged over the domain and the simulation period of 8 - 12 hours: **(a)** N_i, **(b)** N_c, **(c)** Q_i and **(d)** Q_c. The F22 comparison run is plotted in dotted cyan (see dotted line in Fig. 7), S0 in green, S0.5 and S0.75 in blue, S1.25 and S1.5 in yellow. Simulations that yielded significant differences compared to F22 are shown in the respective variable's legend in the subplots **(a)**-**(d)**. Horizontal dashed lines indicate the cloud top and bottom in F22.

230 IWP, N_i and Q_i while a lower variability results in significantly smaller values (Fig. 7 and Fig. 8). The changes are exponential with linear changes of σ, since σ is in the exponent in the INPC RFD (Eq. 1). These results emphasize that it is the high INPCs that dominate ice formation in F22. Ice formation triggered by high INPCs could lead to cloud glaciation and subsequent cloud

https://doi.org/10.5194/acp-2022-696
Preprint. Discussion started: 4 October 2022


Atmospheric Chemistry and Physics Discussions

dissipation in colder clouds, if ice crystals grow on the expense of liquid droplets due to the WBF process. A high N_i can also be relevant for secondary ice processes, where N_i is enhanced by mechanical splintering or break-up of ice crystals (e.g., Field et al., 2016). For example Yano et al. (2016) report a critical $N_{i,\mathrm{crit}}$ which can lead to an explosive enhancement of the number of ice crystals. This $N_{i,\mathrm{crit}}$ might only be reached if there is a possibility to draw high INPCs. If high INPCs become less probable (smaller σ), IWP, N_i and Q_i decrease. This is also apparent when analyzing the simulation without an INPC distribution, using the RFD's median value at all time steps (green line in Figs. 7, 8a and c). All ice-variables (IWP, N_i and Q_i) have the lowest values for this run (see Table 3). So using realistic mean INPCs at the rather high temperature of the simulated case leads to almost no ice formation. Only once an INPC distribution is added, considerable ice is formed. Excluding negative ΔN_i (Eq. 2a) causes N_i to progressively increase even without decreasing cloud temperature. Such increases can be expected from time-dependent immersion freezing.

It is remarkable that the large increase in ice for S1.5 even leads to changes in N_c and Q_c (Fig. 8b and d). The cloud bottom is elevated by ca. 100 m in comparison to the F22 case (Fig. 8b). This is probably because more cloud droplets freeze, leading to a depletion of unfrozen cloud droplets. Within the cloud, N_c is very similar for S1.5 and F22. However, Q_c for S1.5 is significantly smaller, indicating an enhanced WBF process resulting in liquid droplet evaporation.

3.1.3 Size of the temperature bins

For the F22 simulation, we draw from the INPC RFD defined on 1°C temperature bins. Thus a change in temperature from e.g., -10.4 to -10.6°C shifts the INPC from the concentrations at -10°C to the concentrations at -11°C of the INPC distribution. Using smaller temperature bins can be expected to make the parameterization less sensitive to small temperature changes and lead to smaller changes in the drawn INPC concentrations. This effect was tested by decreasing the temperature bins from 1°C to 0.5°C (0.5Deg in Tab. 3). Figure 9 shows the IWP for a run with 0.5°C temperature binning. Overall, IWP for the 0.5Deg simulation does not significantly differ from the F22 runs. Until hour 8, IWP is slightly below the F22 case and between hours 9 and 11, IWP is slightly larger. The averaged profiles for the final four simulated hours are shown in Fig. 10. None of the variables differ significantly between F22 and 0.5Deg (see Tab. 3). Judging from these results, there is no compelling benefit in decreasing the size of the temperature bins.

3.1.4 Frequency of drawing

The frequency of drawing a new value for the INPC simulates the INPC variability over time. The frequency of drawing is coupled to the model's temporal resolution, since the maximum frequency of drawing is restricted by the time step of the model. Considering that one grid box within the cloud has the minimum dimensions of $62.5\ \mathrm{m} \cdot 62.5\ \mathrm{m} \cdot 7.5\ \mathrm{m} \approx 29{,}300\ \mathrm{m}^3$ and that the INP concentration can be assumed to be highly variable on even small time scales (Bigg, 1961) and smaller spatial scales, it is a plausible assumption to modulate INPC in each time step. The sensitivity on drawing frequency was tested by drawing the INPC once every five seconds (5S, see Tab. 3), once every ten seconds (10S), once every 20 seconds (20S), once every five minutes (5M) and once every 60 minutes (60M) instead of at every time step (F22: every 1-3 seconds). Freezing events still occur at every time step, but within the respective time period (e. g. five seconds or 60 minutes), the INPC is constant at

https://doi.org/10.5194/acp-2022-696
Preprint. Discussion started: 4 October 2022

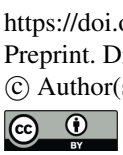

Atmospheric Chemistry and Physics Discussions

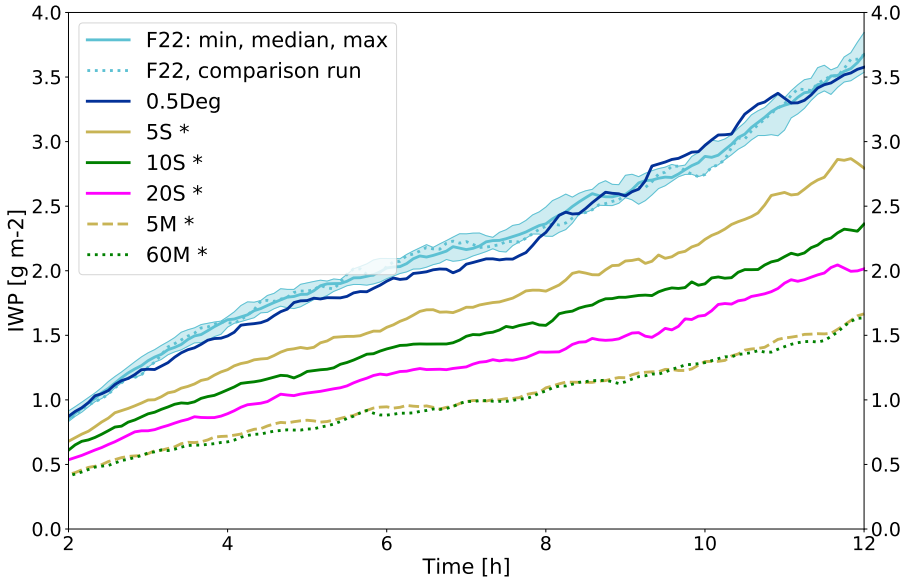

Figure 9. Domain-averaged IWP for 10 F22 simulations (cyan; median with min/max envelope, comparison run used in Fig. 10 is shown as dotted line). Six sensitivity tests (blue: 0.5Deg, yellow solid: 5S, green solid: 10S, magenta solid: 20S, yellow dashed: 5M, green dotted: 60M). Significant differences to F22 are marked with an asterisk.

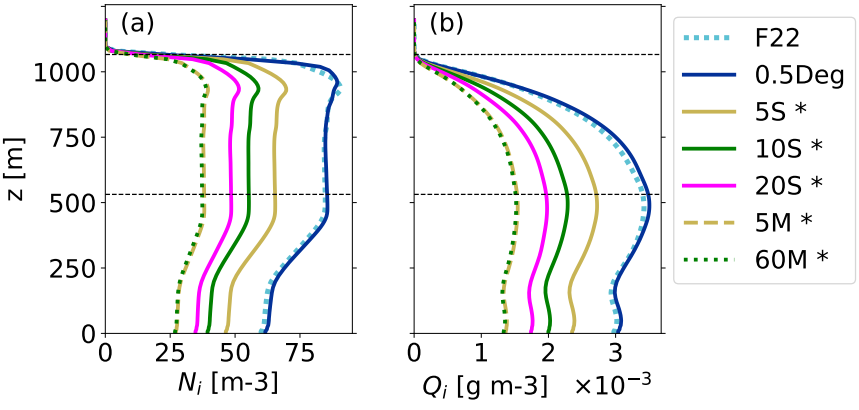

Figure 10. Profiles averaged over the domain and the simulation period of 8 - 12 hours: **(a)** N_i, **(b)** Q_i. One F22 run in dotted cyan (see dotted line in Fig. 9), 0.5Deg in blue, 5S in yellow solid, 10S in green solid, 20S in magenta solid, 5M in yellow dashed, 60M in green dotted. Simulations with significant differences compared to F22 are marked with an asterisk. Horizontal dashed lines indicate the cloud top and bottom in F22.

one grid point for the time period. If the temperature at the grid point changes before the completion of the time period, a new INPC is drawn earlier.

https://doi.org/10.5194/acp-2022-696
Preprint. Discussion started: 4 October 2022

Atmospheric Chemistry and Physics Discussions

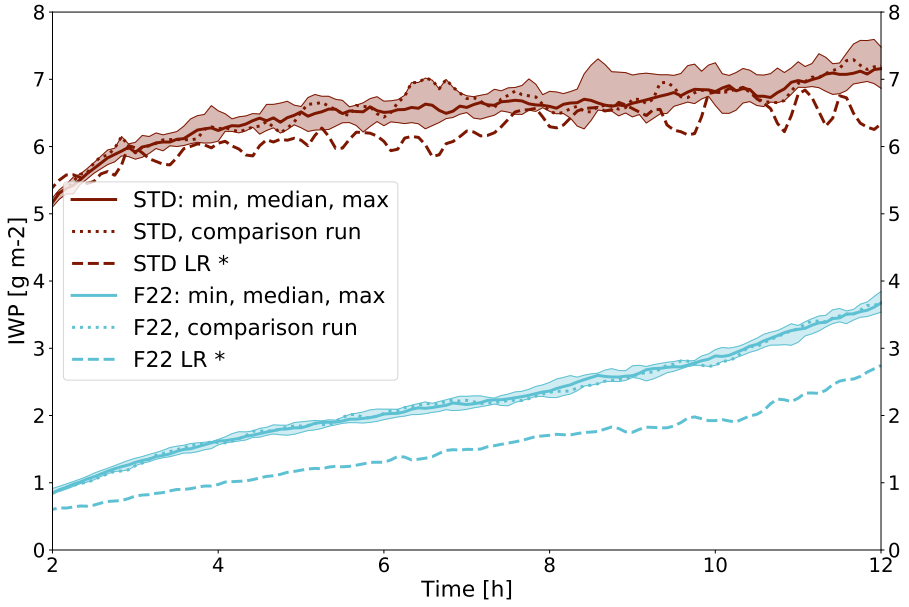

Figure 11. Domain-averaged IWP for 10 STD (red; median with min/max envelope, comparison run used in Fig. 12 is shown as dotted line) and 10 F22 simulations (cyan; median with min/max envelope, comparison run used in Fig. 12 is shown as dotted line). One run with half of entire resolution respectively (dashed lines). Significant differences to STD or F22 are marked with an asterisk.

IWP, N_i and Q_i for the runs with lower drawing frequencies exhibit similar relative N_i increase over time as F22, but have significantly lower absolute N_i concentrations (Figs. 9 and 10). The ice variables decrease as the frequency of drawing decreases. This evolution can be explained by the subtraction of N_i at each time step. N_i at a grid point will not change between time steps for which INPC $< N_i$. Only when a newly drawn INPC $> N_i$, new ice is formed at the grid point. An exception is if there is a sink for N_i at the grid point (e.g., sedimentation, aggregation, advection) and N_i becomes smaller than INPC before the next draw of INPC, since then INPC - N_i cloud droplets will freeze. As the overall chances of drawing INPC $> N_i$ is higher with higher drawing frequency, the frequency of drawing new INPCs changes the amount of new ice formation and ice content in the cloud. Another feature apparent in Figs. 9 and 10, as well as Tab. 3 is that the ice variables converge for drawing frequencies of five minutes or larger. This is likely the average time it takes for temperature to change at the grid points for the simulated stratiform cloud. The sensitivity to drawing frequency may be different for different cloud types. For example, in convective clouds the sensitivity could be very low because the temperature changes more quickly than in the presented stratiform cloud, which leads to a high frequency of draws no matter which drawing frequency is chosen in the scheme.

3.1.5 Resolution of the domain

The spatial resolution of the model domain affects the F22 scheme in a similar way as the frequency of drawing, by changing the number of draws of INPC for the same cloud. However, a change in the model resolution impacts all parts of the model,

https://doi.org/10.5194/acp-2022-696
Preprint. Discussion started: 4 October 2022

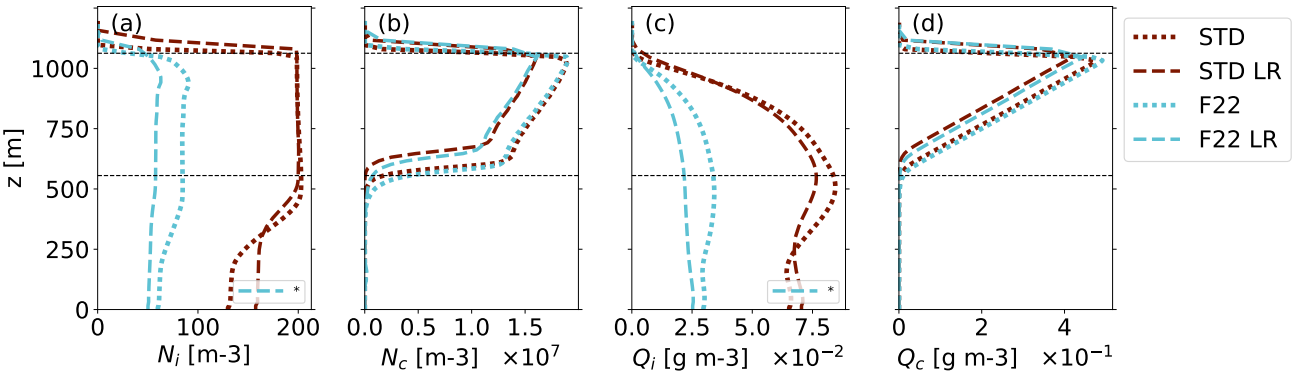

Figure 12. Profiles averaged over the domain and the simulation period of 8 - 12 hours: **(a)** N_i, **(b)** N_c, **(c)** Q_i and **(d)** Q_c. One STD in red dotted, one F22 run in cyan dotted (see dotted lines in Fig. 11), STD LR in red dashed and F22 LR in cyan dashed. Simulations that yielded significant differences compared to F22 are shown in the respective variable's legend. Horizontal dashed lines indicate the cloud top and bottom in STD.

including microphysical processes. The sensitivity of the LES at lower resolution is tested by doubling the grid spacing in all three dimensions while the domain volume remains constant (STD LR and F22 LR). Note that this will also lead to a doubling of the model time step, since it is calculated dynamically to satisfy the CFL criterion. Testing the scheme on a more coarse grid is important, since the goal for the new parameterization is that it can be used in larger-scale models where the resolution will be much coarser than in large-eddy simulations. Lowering the resolution leads to significantly lower IWP for both the STD LR and F22 LR simulation (Fig. 11). IWP is affected more in the simulation with the F22 scheme. The vertical profiles of the cloud droplet variables (Figs. 12b and d) show non-significant, but consistent decreases in N_c (Fig. 12b), as well as Q_c (Fig. 12d) for both runs with lower resolution. The decrease might be caused by changes in mixing processes, e.g., entrainment at the cloud borders, due to the change in grid size. N_i within the cloud is fixed to 200 m^{-3} for STD LR and STD (Fig. 12a). Nevertheless, Q_i is lower for STD LR compared to STD (Fig. 12c). This can be explained by the decrease in Q_c and thus a less efficient WBF process providing a smaller mass flux from liquid droplets to ice crystals. For F22 LR, all variables shown in Fig. 12 decrease - for N_i and Q_i these changes are significant. The decrease in N_i can be explained by the smaller number of grid points in the domain. INPCs will be drawn at only one eighth of the number of grid points in F22 LR and thus large INPCs will be picked less often than for F22. The results shown in Figs. 11 and 12 underline the conclusion from Sec. 3.1.2 that the highest INPCs have the strongest effect on overall N_i.

4 Conclusions

A novel parameterization of immersion freezing that takes into account observed variability of ice nucleating particles is presented. The observed INPC variability is reproduced by random drawing from an INPC relative frequency distribution that

https://doi.org/10.5194/acp-2022-696
Preprint. Discussion started: 4 October 2022


Atmospheric Chemistry and Physics Discussions

depends on temperature. Since the F22 parameterization is based on long-term and wide-spread atmospheric INPC observations in a broad temperature range, it is valid for the entire temperature range of heterogeneous immersion freezing between 0 and -38°C. F22 has the additional advantage that it does not require information on the present bulk aerosol from the atmospheric model, which makes it easy to implement and use in many different models.

We tested the parameterization for the simulation of a mixed-phase Arctic stratocumulus cloud case with MIMICA. We used this case as a test bed for F22 because aerosol characteristics in the Arctic are largely unknown and this lack of information on aerosol bulk properties makes it challenging to use "classical" aerosol-based freezing schemes. Moreover, it might be important to consider the whole range of possible INPCs in the Arctic summer where warm mixed-phase clouds are frequently observed. It was found that the simulated IWP, N_i and Q_i of the cloud depend linearly on the median of the relative frequency distribution that describes the INPC variability, and exponentially on the distribution's standard deviation. The large dependency on the standard deviation of the distribution is especially interesting, as it implies that the amount of ice in the modeled cloud is particularly sensitive to high INP concentrations. The possibility of drawing high INPC can influence cloud glaciation for colder cases caused by the WBF process and secondary ice processes when $N_{i,\mathrm{crit}}$ is reached (Yano et al., 2016). The relevance of randomly drawing INPC from a distribution is highlighted by the much lower IWP, N_i and Q_i when simply using the median INP concentration (i.e., no INPC distribution). In addition to the distribution's median and standard deviation, the frequency of drawing a new INPC has a significant impact on the ice variables, since it is when a new INPC is drawn that most ice is formed (Eq. 2a). The lower the frequency of drawing, the lower the ice content in the cloud. However, drawing every five minutes or less often (e.g., every 60 minutes) leads to a similar amount of ice in the cloud. This saturation effect depends on the modeled cloud type and the temperature fluctuations within the cloud. Lower resolution of the model domain affects both the ice and cloud droplet concentrations within the cloud, as well as mixing ratios. This sensitivity should be considered for possible implementations of the scheme into models with different resolutions.

A qualitative comparison with similar simulations (ASCOS in MIMICA) by Sotiropoulou et al. (2021) or Stevens et al. (2018) shows slightly lower IWP for the baseline F22 setup. In contrast to the two studies, we have not included graupel and snow in our simulations, thus we expect lower IWP. This means that our results are in a reasonable range with previous studies.

The scheme's independence from aerosol information in the atmospheric model is a strength, but can be a limitation. F22 represents the measurements (in this case maritime background measurements) behind the given INPC RFD that may not be representative for distinct scenarios, e.g., a Sahara dust outbreak. The RFD would need to be updated with one that is based on INPC observations specific for the event or location. However, the parameterization is flexible to be adapted to different sets of observational INPC from other locations or years. To represent several sources or source regions at the same time in a model, different RFDs could be used depending on the location (remote vs. continental INP as an example). The independence to modeled aerosol might require updating the RFD when simulating future scenarios including changes in aerosol or INP concentrations. Some degree of autocorrelation between subsequent random draws from the INPC RFD in time and space could be added to the scheme in the future. It is not clear what degree of autocorrelation would be physically reasonable. Since our study is based on one rather warm Arctic stratocumulus case, the parameterization should be tested and validated for other conditions and case studies in the future, especially for lower in-cloud temperatures. Additionally, it should be tested how F22

https://doi.org/10.5194/acp-2022-696
Preprint. Discussion started: 4 October 2022


Atmospheric Chemistry and Physics Discussions

performs in LES-models other than MIMICA, or larger scale models. The intention of this study was to learn what including randomness in INPC can lead to. We showed that representing INP heterogeneity in an immersion freezing parameterization allows for a realistic simulation of an Arctic stratocumulus cloud.

In order to make it easier to use INPC observations in schemes like the one presented, measurements should be reported either as individual measurements points (e.g., as time series), or if aggregated both with the average and standard deviation of the underlying log-normal distribution.

Code and data availability. The model output data presented in this study will be published at Zenodo after acceptance of the paper. Fortran code for the scheme is available from the authors upon request.

Author contributions. **Idea**: AW, LI **Prestudy**: ML, AW, LI **Conceptualisation**: LI, HF **Model implementation**: HF **Simulations**: HF **Analysis of the data and visualisation**: HF, LI **Writing**: HF **Review & editing**: All authors.

Competing interests. The authors declare that no competing interests are present.

Acknowledgements. H.C.F. and L.I. were supported by Chalmers Gender Initiative for Excellence (Genie). E.S.T. was supported by the Swedish Research Councils, FORMAS (2017-00564) and VR (2020-03497) and the Swedish Strategic Research Initiative MERGE. The computations were enabled by resources provided by the Swedish National Infrastructure for Computing (SNIC) at National Supercomputer Centre (NSC) partially funded by the Swedish Research Council through grant agreement no. 2018-05973. Hamish Struthers at LiU is acknowledged for assistance concerning technical and implementational aspects in making the code run on the Tetralith resources. We thank Annica M. L. Ekman for valuable discussions. We used the colormaps provided by Crameri et al. (2020).

https://doi.org/10.5194/acp-2022-696
Preprint. Discussion started: 4 October 2022

Atmospheric Chemistry and Physics Discussions

References

Bertrand, J., Baudet, J., and Dessens, J.: Seasonal Variations and Frequency Distributions of Ice Nuclei Concentrations at Abidjan, West Africa, J. Appl. Meteorol. Climatol., 12, 1191–1195, https://doi.org/10.1175/1520-0450(1973)012<1191:SVAFDO>2.0.CO;2, 1973.

Bigg, E. K.: Natural Atmospheric Ice Nuclei, Sci. Prog., 49, 458–475, http://www.jstor.org/stable/43425202, 1961.

Bulatovic, I., Igel, A. L., Leck, C., Heintzenberg, J., Riipinen, I., and Ekman, A. M.: The Importance of Aitken Mode Aerosol Particles for Cloud Sustenance in the Summertime High Arctic-A Simulation Study Supported by Observational Data, Atmospheric Chem. Phys., 21, 3871–3897, https://doi.org/10.5194/acp-21-3871-2021, 2021.

Burrows, S. M., McCluskey, C. S., Cornwell, G., Steinke, I., Zhang, K., Zhao, B., Zawadowicz, M., Raman, A., Kulkarni, G., China, S., Zelenyuk, A., and DeMott, P. J.: Ice-Nucleating Particles That Impact Clouds and Climate: Observational and Modeling Research Needs, Rev. Geophys., 60, e2021RG000 745, https://doi.org/10.1029/2021RG000745, 2022.

Christiansen, S., Ickes, L., Bulatovic, I., Leck, C., Murray, B. J., Bertram, A. K., Wagner, R., Gorokhova, E., Salter, M. E., Ekman, A. M., and Bilde, M.: Influence of Arctic Microlayers and Algal Cultures on Sea Spray Hygroscopicity and the Possible Implications for Mixed-Phase Clouds, J. Geophys. Res. Atmospheres, 125, https://doi.org/10.1029/2020JD032808, 2020.

Conen, F., Yakutin, M. V., Yttri, K. E., and Hüglin, C.: Ice Nucleating Particle Concentrations Increase When Leaves Fall in Autumn, Atmosphere, 8, 202, https://doi.org/10.3390/atmos8100202, 2017.

Crameri, F., Shephard, G. E., and Heron, P. J.: The misuse of colour in science communication, Nat. Commun., 11, 5444, https://doi.org/10.1038/s41467-020-19160-7, 2020.

Field, P. R., Lawson, R. P., Brown, P. R. A., Lloyd, G., Westbrook, C., Moisseev, D., Miltenberger, A., Nenes, A., Blyth, A., Choularton, T., Connolly, P., Buehl, J., Crosier, J., Cui, Z., Dearden, C., DeMott, P., Flossmann, A., Heymsfield, A., Huang, Y., Kalesse, H., Kanji, Z. A., Korolev, A., Kirchgaessner, A., Lasher-Trapp, S., Leisner, T., McFarquhar, G., Phillips, V., Stith, J., and Sullivan, S.: Chapter 7. Secondary Ice Production - Current State of the Science and Recommendations for the Future, Meteorol. Monogr., pp. AMSMONOGRAPHS–D–16–0014.1, https://doi.org/10.1175/AMSMONOGRAPHS-D-16-0014.1, 2016.

Fletcher, N.: The physics of rainclouds, Cambridge University Press, 1962.

Flyger, H. and Heidam, N. Z.: Ground Level Measurements of the Summer Tropospheric Aerosol in Northern Greenland, Journal of Aerosol Science, 9, 157–168, https://doi.org/10.1016/0021-8502(78)90075-7, 1978.

Fu, Q. and Liou, K. N.: Parameterization of the Radiative Properties of Cirrus Clouds, J. Atmospheric Sci., 50, 2008–2025, 1993.

Hartmann, M., Blunier, T., Brügger, S., Schmale, J., Schwikowski, M., Vogel, A., Wex, H., and Stratmann, F.: Variation of Ice Nucleating Particles in the European Arctic Over the Last Centuries, Geophys. Res. Lett., 46, 4007–4016, https://doi.org/10.1029/2019GL082311, 2019.

Ickes, L., Welti, A., and Lohmann, U.: Classical Nucleation Theory of Immersion Freezing: Sensitivity of Contact Angle Schemes to Thermodynamic and Kinetic Parameters, Atmospheric Chem. Phys., 17, 1713–1739, https://doi.org/10.5194/acp-17-1713-2017, 2017.

Isaac, G. A. and Douglas, R. H.: Frequency Distributions of Ice Nucleus Concentrations, J. Rech. Atmos., 5, 1–4, 1971.

Khvorostyanov, V. I. and Curry, J. A.: A New Theory of Heterogeneous Ice Nucleation for Application in Cloud and Climate Models, Geophys. Res. Lett., 27, 4081–4084, https://doi.org/10.1029/1999GL011211, 2000.

Khvorostyanov, V. I. and Curry, J. A.: Aerosol Size Spectra and CCN Activity Spectra: Reconciling the Lognormal, Algebraic, and Power Laws, J. Geophys. Res., 111, D12 202, https://doi.org/10.1029/2005JD006532, 2006.

https://doi.org/10.5194/acp-2022-696
Preprint. Discussion started: 4 October 2022

Atmospheric Chemistry and Physics Discussions

Li, G., Wieder, J., Pasquier, J. T., Henneberger, J., and Kanji, Z. A.: Predicting Atmospheric Background Number Concentration of Ice Nucleating Particles in the Arctic, Atmospheric Chem. Phys. Discuss., pp. 1–27, https://doi.org/10.5194/acp-2022-21, under review, 2022.

Loewe, K., Ekman, A. M. L., Paukert, M., Sedlar, J., Tjernström, M., and Hoose, C.: Modelling Micro- and Macrophysical Contributors to the Dissipation of an Arctic Mixed-Phase Cloud during the Arctic Summer Cloud Ocean Study (ASCOS), Atmospheric Chem. Phys., 17, 6693–6704, https://doi.org/10.5194/acp-17-6693-2017, 2017.

Marcolli, C., Gedamke, S., Peter, T., and Zobrist, B.: Efficiency of Immersion Mode Ice Nucleation on Surrogates of Mineral Dust, Atmos. Chem. Phys., 7, 5081–5091, https://doi.org/10.5194/acp-7-5081-2007, 2007.

Matus, A. V. and L'Ecuyer, T. S.: The role of cloud phase in Earth's radiation budget, J. Geophys. Res. Atmos., 122, 2559–2578, https://doi.org/10.1002/2016JD025951, 2017.

Morrison, H. and Grabowski, W. W.: Modeling Supersaturation and Subgrid-Scale Mixing with Two-Moment Bulk Warm Microphysics, J. Atmospheric Sci., 65, 792–812, https://doi.org/10.1175/2007JAS2374.1, 2008.

Niemand, M., Möhler, O., Vogel, B., Vogel, H., Hoose, C., Connolly, P., Klein, H., Bingemer, H., Demott, P., Skrotzki, J., and Leisner, T.: A Particle-Surface-Area-Based Parameterization of Immersion Freezing on Desert Dust Particles, J. Atmospheric Sci., 69, 3077–3092, https://doi.org/10.1175/JAS-D-11-0249.1, 2012.

Ott, W. R.: A Physical Explanation of the Lognormality of Pollutant Concentrations, J. Air Waste Manag. Assoc., 40, 1378–1383, https://doi.org/10.1080/10473289.1990.10466789, 1990.

Petters, M. D. and Wright, T. P.: Revisiting Ice Nucleation from Precipitation Samples, Geophys. Res. Lett., 42, 8758–8766, https://doi.org/10.1002/2015GL065733, 2015.

Phillips, V. T. J., DeMott, P. J., and Andronache, C.: An Empirical Parameterization of Heterogeneous Ice Nucleation for Multiple Chemical Species of Aerosol, J. Atmos. Sci., 65, 2757–2783, https://doi.org/10.1175/2007JAS2546.1, 2008.

Radke, L. F., Hobbs, P. V., and Pinnons, J. E.: Observations of Cloud Condensation Nuclei, Sodium-Containing Particles, Ice Nuclei and the Light-Scattering Coefficient Near Barrow, Alaska, J. Appl. Meteorol. Climatol., 15, 982–995, https://doi.org/10.1175/1520-0450(1976)015<0982:OOCCNS>2.0.CO;2, 1976.

Savre, J. and Ekman, A. M.: A Theory-Based Parameterization for Heterogeneous Ice Nucleation and Implications for the Simulation of Ice Processes in Atmospheric Models, J. Geophys. Res., 120, 4937–4961, https://doi.org/10.1002/2014JD023000, 2015a.

Savre, J. and Ekman, A. M. L.: Large-Eddy Simulation of Three Mixed-Phase Cloud Events during ISDAC: Conditions for Persistent Heterogeneous Ice Formation, J. Geophys. Res. Atmospheres, 120, 7699–7725, https://doi.org/10.1002/2014JD023006, 2015b.

Savre, J., Ekman, A. M. L., and Svensson, G.: Technical Note: Introduction to MIMICA, a Large-Eddy Simulation Solver for Cloudy Planetary Boundary Layers, J. Adv. Model. Earth Syst., 6, 630–649, https://doi.org/10.1002/2013MS000292, 2014.

Schrod, J., Thomson, E. S., Weber, D., Kossmann, J., Pöhlker, C., Saturno, J., Ditas, F., Artaxo, P., Clouard, V., Saurel, J.-M., Ebert, M., Curtius, J., and Bingemer, H. G.: Long-Term Deposition and Condensation Ice-Nucleating Particle Measurements from Four Stations across the Globe, Atmos. Chem. Phys., 20, 15 983–16 006, https://doi.org/10.5194/acp-20-15983-2020, 2020.

Seifert, A. and Beheng, K. D.: A Double-Moment Parameterization for Simulating Autoconversion, Accretion and Selfcollection, Atmospheric Res., https://doi.org/10.1016/S0169-8095(01)00126-0, 2001.

Seifert, A. and Beheng, K. D.: A Two-Moment Cloud Microphysics Parameterization for Mixed-Phase Clouds. Part 1: Model Description, Meteorol. Atmospheric Phys., 92, 45–66, https://doi.org/10.1007/s00703-005-0112-4, 2006.

Solomon, A., Feingold, G., and Shupe, M. D.: The Role of Ice Nuclei Recycling in the Maintenance of Cloud Ice in Arctic Mixed-Phase Stratocumulus, Atmospheric Chem. Phys., 15, 10 631–10 643, https://doi.org/10.5194/acp-15-10631-2015, 2015.

https://doi.org/10.5194/acp-2022-696
Preprint. Discussion started: 4 October 2022

Sotiropoulou, G., Sullivan, S., Savre, J., Lloyd, G., Lachlan-Cope, T., Ekman, A. M. L., and Nenes, A.: The Impact of Secondary Ice Production on Arctic Stratocumulus, Atmospheric Chem. Phys., 20, 1301–1316, https://doi.org/10.5194/acp-20-1301-2020, 2020.

Sotiropoulou, G., Ickes, L., Nenes, A., and Ekman, A. M. L.: Ice Multiplication from Ice–Ice Collisions in the High Arctic: Sensitivity to Ice Habit, Rimed Fraction, Ice Type and Uncertainties in the Numerical Description of the Process, Atmospheric Chem. Phys., 21, 9741–9760, https://doi.org/10.5194/acp-21-9741-2021, 2021.

Stevens, R. G., Loewe, K., Dearden, C., Dimitrelos, A., Possner, A., Eirund, G. K., Raatikainen, T., Hill, A. A., Shipway, B. J., Wilkinson, J., Romakkaniemi, S., Tonttila, J., Laaksonen, A., Korhonen, H., Connolly, P., Lohmann, U., Hoose, C., Ekman, A. M. L., Carslaw, K. S., and Field, P. R.: A Model Intercomparison of CCN-limited Tenuous Clouds in the High Arctic, Atmospheric Chem. Phys., 18, 11 041–11 071, https://doi.org/10.5194/acp-18-11041-2018, 2018.

Tjernström, M., Birch, C. E., Brooks, I. M., Shupe, M. D., Persson, P. O. G., Sedlar, J., Mauritsen, T., Leck, C., Paatero, J., Szczodrak, M., and Wheeler, C. R.: Meteorological Conditions in the Central Arctic Summer during the Arctic Summer Cloud Ocean Study (ASCOS), Atmospheric Chem. Phys., 12, 6863–6889, https://doi.org/10.5194/acp-12-6863-2012, 2012.

Tjernström, M., Leck, C., Birch, C. E., Bottenheim, J. W., Brooks, B. J., Brooks, I. M., Bäcklin, L., Chang, R. Y.-W., de Leeuw, G., Di Liberto, L., de la Rosa, S., Granath, E., Graus, M., Hansel, A., Heintzenberg, J., Held, A., Hind, A., Johnston, P., Knulst, J., Martin, M., Matrai, P. A., Mauritsen, T., Müller, M., Norris, S. J., Orellana, M. V., Orsini, D. A., Paatero, J., Persson, P. O. G., Gao, Q., Rauschenberg, C., Ristovski, Z., Sedlar, J., Shupe, M. D., Sierau, B., Sirevaag, A., Sjogren, S., Stetzer, O., Swietlicki, E., Szczodrak, M., Vaattovaara, P., Wahlberg, N., Westberg, M., and Wheeler, C. R.: The Arctic Summer Cloud Ocean Study (ASCOS): Overview and Experimental Design, Atmospheric Chem. Phys., 14, 2823–2869, https://doi.org/10.5194/acp-14-2823-2014, 2014.

Vali, G., DeMott, P. J., Möhler, O., and Whale, T. F.: Technical Note: A Proposal for Ice Nucleation Terminology, Atmospheric Chem. Phys., 15, 10 263–10 270, https://doi.org/10.5194/acp-15-10263-2015, 2015.

Wang, C. and Chang, J. S.: A Three-Dimensional Numerical Model of Cloud Dynamics, Microphysics, and Chemistry: 1. Concepts and Formulation, J. Geophys. Res., 98, 14 827, https://doi.org/10.1029/92JD01393, 1993.

Wang, Y., Liu, X., Hoose, C., and Wang, B.: Different Contact Angle Distributions for Heterogeneous Ice Nucleation in the Community Atmospheric Model Version 5, Atmospheric Chem. Phys., 14, 10 411–10 430, https://doi.org/10.5194/acp-14-10411-2014, 2014.

Welti, A., Müller, K., Fleming, Z. L., and Stratmann, F.: Concentration and Variability of Ice Nuclei in the Subtropical Maritime Boundary Layer, Atmospheric Chem. Phys., 18, https://doi.org/10.5194/acp-18-5307-2018, 2018.

Welti, A., Bigg, E. K., DeMott, P., Gong, X., Hartmann, M., Harvey, M., Henning, S., Herenz, P., Hill, T., Hornblow, B., Leck, C., Löffler, M., McCluskey, C., Rauker, A. M., Schmale, J., Tatzelt, C., van Pinxteren, M., and Stratmann, F.: Ship-Based Measurements of Ice Nuclei Concentrations over the Arctic, Atlantic, Pacific and Southern Ocean, Atmospheric Chem. Phys., pp. 1–22, https://doi.org/10.5194/acp-2020-466, 2020.

Wex, H., Huang, L., Zhang, W., Hung, H., Traversi, R., Becagli, S., Sheesley, R. J., Moffett, C. E., Barrett, T. E., Bossi, R., Skov, H., Hünerbein, A., Lubitz, J., Löffler, M., Linke, O., Hartmann, M., Herenz, P., and Stratmann, F.: Annual Variability of Ice-Nucleating Particle Concentrations at Different Arctic Locations, Atmospheric Chem. Phys., 19, 5293–5311, https://doi.org/10.5194/acp-19-5293-2019, 2019.

Yano, J.-I., Phillips, V. T. J., and Kanawade, V.: Explosive Ice Multiplication by Mechanical Break-up in Ice–Ice Collisions: A Dynamical System-Based Study, Q. J. R. Meteorol. Soc., 142, 867–879, https://doi.org/10.1002/qj.2687, 2016.

https://doi.org/10.5194/acp-2022-696
Preprint. Discussion started: 4 October 2022

Atmospheric Chemistry and Physics Discussions

Appendix A: MIMICA LES model description

The MIMICA LES solves a system of non-hydrostatic anelastic equations and represents cloud microphysics through a two-moment bulk microphysics scheme. The prognostic variables are number concentrations and mass mixing ratios of up to five represented hydrometeors: cloud droplets, rain drops, cloud ice, snow, and graupel. All hydrometeor mass distributions are regular gamma-distributions and the hydrometeors' terminal fall speeds are calculated from simple power laws dependent on their diameters. Warm microphysical processes are modeled according to Seifert and Beheng (2001) and Seifert and Beheng (2006), while collection processes involving frozen hydrometeors and resulting in the hydrometeors sticking together follow Wang and Chang (1993). MIMICA represents the following cold collection processes: i. riming of ice crystals and graupel by cloud droplets (resulting in graupel); ii. riming of ice crystals, graupel and snow flakes by rain drops (resulting in graupel); iii. autoconversion of ice crystals to snow; iv. self-collection of snow flakes; v. collection of cloud droplets by snow (resulting in snow); vi. growth of a snow flake by aggregating ice crystals; vii. collection of snow by graupel (resulting in graupel). Cloud condensation nuclei (CCN) activation is described following Khvorostyanov and Curry (2006), which is based on a simple power-law depending on modeled supersaturation and a prescribed background CCN concentration. It is possible to describe aerosol prognostically in MIMICA including activation as CCN. The supersaturation is solved pseudo-analytically following Morrison and Grabowski (2008). In the standard version of MIMICA, primary ice formation is represented by maintaining a constant ice crystal number concentration (N_i) within the cloud. However, it is also possible to choose an interactive ice nucleation scheme. Secondary ice formation is not taken into account in this study since the focus is on primary ice formation. Radiation is calculated according to Fu and Liou (1993). The initial ice/liquid potential temperature profiles are randomly perturbed in order for convection to develop quicker. Consequently, any two simulations will yield different results, even if all parameters are held constant.

Appendix B: Averaged profiles for STD vs. F22

Figure B1 shows time- and domain-averaged profiles of the number concentrations and mixing ratios of ice and cloud droplets.

https://doi.org/10.5194/acp-2022-696
Preprint. Discussion started: 4 October 2022

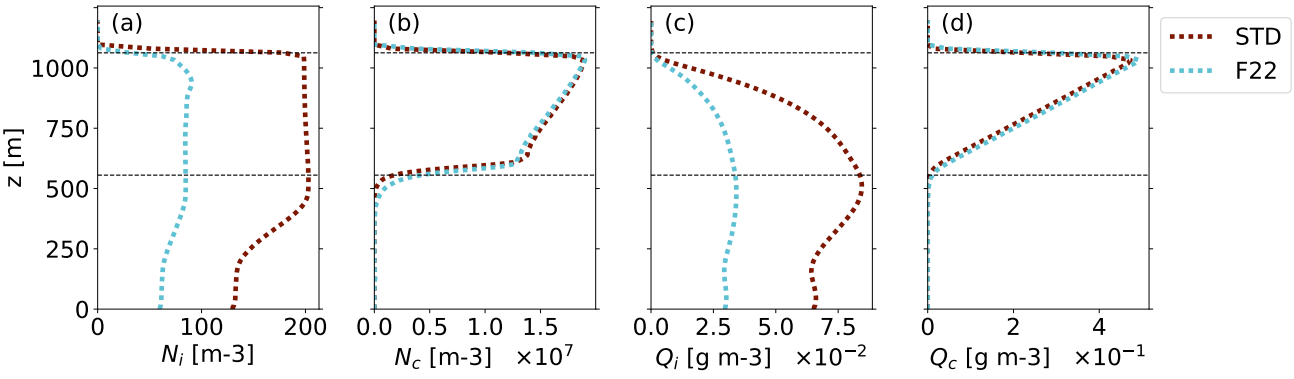

Figure B1. Profiles averaged over the domain and the simulation period of 8 - 12 hours: **(a)** N_i, **(b)** N_c, **(c)** Q_i and **(d)** Q_c. One STD in red dotted, one F22 run in cyan dotted (see dotted lines in Fig. 3). Horizontal dashed lines indicate the cloud top and bottom in STD.